

Modelling Excitable Cells Using Cycle-Linear Hybrid Automata

Journal:	<i>IET Systems Biology</i>
Manuscript ID:	SYB-2007-0001
Manuscript Type:	Original Manuscript
Date Submitted by the Author:	02-Jan-2007
Complete List of Authors:	Ye, Pei; SUNY at Stony Brook, Computer Sciences Entcheva, Emilia; SUNY at Stony Brook, BME department Smolka, Scott; SUNY at Stony Brook, Computer Sciences department Grosu, Radu; SUNY at Stony Brook, Computer Sciences department
Keyword:	excitable cell, hybrid automata, cycle-linear hybrid automata



Modelling Excitable Cells Using Cycle-Linear Hybrid Automata

P. Ye* E. Entcheva† S.A. Smolka*
R. Grosu*

* Computer Science Department, SUNY at Stony Brook, Stony Brook, NY, 11794, U.S.A.

{pye, sas, grosu}@cs.sunysb.edu

†Biomedical Engineering Department, SUNY at Stony Brook, Stony Brook, NY, 11794, U.S.A.

Emilia.Entcheva@sunysb.edu

Abstract

In this paper, we introduce Cycle-Linear Hybrid Automata (CLHA), a novel model of excitable cells that efficiently and accurately captures action-potential morphology and other typical excitable-cell characteristics such as refractoriness and restitution. Hybrid automata combine discrete transition graphs with continuous dynamics, and emerge in a natural way during the (piecewise) approximation process of any nonlinear system. CLHA are a new form of Hybrid automata that exhibit linear behavior on a per-cycle basis but whose overall behavior is appropriately nonlinear. To motivate the need for this modelling formalism, we first show how to recast two recently proposed models of excitable cells as hybrid automata: the piecewise-linear model of Biktashev and the nonlinear model of Fenton-Karma. Both of these models were designed to efficiently approximate excitable-cell behavior. We then show that our CLHA model closely mimics the behavior of several classical highly nonlinear models of excitable cells, thereby retaining the simplicity of Biktashev's model without sacrificing the expressiveness of Fenton-Karma. CLHA are not restricted to excitable cells; they can be used to model a wide class of dynamic systems that exhibits some level of periodicity plus adaptation.

1 Introduction

Hybrid automata [17] are an increasingly popular modelling formalism for systems that exhibit both continuous and discrete behavior. Intuitively, a hybrid automaton is an extended finite-state automaton, the states of which encode the various phases of continuous dynamics a system may undergo, and the transitions of which are used to express the switching logic between these

dynamics. Hybrid automata are well suited as a computational model for continuous-discrete systems as they (i) possess an intuitive graphical representation; (ii) can be used in a natural way to achieve a piecewise, possibly linear, approximation of any nonlinear system; and (iii) facilitate formal analysis due to their automata-theoretic nature.

Traditionally, hybrid automata have been used to model embedded systems, including automated highway systems [28, 9], air traffic management [19, 21], embedded automotive controllers [4], robotics [2] and real-time circuits. [22]. More recently, they are being used to formally model molecular, intra-cellular, and inter-cellular biological processes [15]. Many biological systems are “hybrid” in nature: biochemical concentrations may vary continuously, yet discrete transitions between distinct states are also possible.

Excitable cells are a good example of biologically inspired hybrid systems: transmembrane ion fluxes and voltages may vary continuously but the transition from the resting state to the excited state is generally considered an all-or-nothing discrete response. Furthermore, networks of genes, molecules and cells tend to exhibit properties such as concurrency and communication, for which automata-based formalisms are well developed [24].

Currently, the preferred modelling approach for biological systems uses large sets of coupled nonlinear differential equations, and analysis is reduced to simulation via numerical techniques. In contrast, models based on hybrid automata provide piecewise, typically linear, approximations, which lead to conceptually simpler models and the possibility for large-scale simulation and formal analysis.

In this paper, we introduce **cycle-linear hybrid automata** (CLHA), a novel model for excitable cells that efficiently and accurately captures both action-potential morphology and typical excitable-cell characteristics such as refractoriness and restitution. The motivation behind the CLHA model is the observation that, during an action potential, an excitable cell cycles through four basic modes of operation—resting, stimulated, early repolarization, final repolarization—and the dynamics of each mode is essentially linear and time-invariant (LTI). To capture frequency-dependent properties such as restitution, the CLHA model is equipped with a one-cycle memory of the cell’s voltage and the per-mode parameters of the current cycle’s LTI system of differential equations are updated according to this voltage. Consequently, the model’s behavior is linear in any one cycle but appropriately nonlinear overall.

To motivate the need for CLHA, we first show how to recast two recently proposed models of excitable cells as hybrid automata: the piecewise-linear model of Biktashev [6] and the nonlinear model of Fenton-Karma [13]. Both of these models were designed to efficiently approximate excitable-cell behavior. We then show that our CLHA model closely mimics the behavior, in terms

of action-potential morphology and frequency-dependent restitution, of several classical highly non-linear models of excitable cells: Hodgkin-Huxley [18], dynamic Luo-Rudy [20], and neonatal rat [11]. One may thus conclude that CLHA, as a formal model of excitable cells, retain the simplicity of Biktashev's model without sacrificing the expressiveness of Fenton-Karma. CLHA are not restricted to excitable cells; they can be advantageously used to model any dynamical system that exhibits some level of periodicity plus adaptation.

The rest of the paper is organized as follows. Section 2 discusses related work. Section 3 defines hybrid automata. Section 4 provides the requisite biological background for excitable cells. Section 5 shows how to recast existing computational models of excitable cells as HA using the Heaviside function for discrete control. Section 6 presents our CLHA model while Section 7 shows how it can be used to efficiently model the action potential and associated frequency-dependent properties of different excitable cells. Section 8 summarizes this work and discusses future research.

2 Related Work

As discussed in the previous section, hybrid automata (HA) are finding more and more use as a modelling formalism for molecular, intra-cellular, and inter-cellular biological processes. In [15], an HA model of a protein-regulatory network is derived by identifying the major modes of operation and the manner in which the network switches between modes. Each of two interacting proteins is associated with two modes: active and non-active. In each mode, a linear dynamic function is used to describe the concentration change of that protein. HA models constructed in this fashion tend to be of low complexity as well as low precision, but may facilitate large-scale simulation and analysis.

Alternatively, a system of coupled nonlinear ordinary differential equations (ODEs) describing processes with disparate time scales can be simplified and transformed into an HA model. This is the approach taken by Biktashev in [6], where a Heaviside function is substituted for a fast-transitioning continuous function, along with certain assumptions about variables remaining constant within a mode [6].

Antoniotti et al. [3] advocate an empirical approach for deriving HA models of biochemical systems from experimental data. In their approach, each time step is associated with a mode. If the data set is large, so is the resulting automaton. Simplification techniques based on "state collapsing" can be used to reduce the number of states, making this method feasible for real applications.

Once a valid HA model has been developed for a biological system, it can be used to explore the

system's parameter space; moreover, formal analysis can be conducted on it. Of particular interest for dynamical systems are **reachability** and **stability** analysis. The former allows one to check whether the transient behavior of the HA contains undesired modes of operation [1, 16]. The latter allows one to check if the the HA, in steady state, exhibits unstable (or chaotic) behavior [10, 5]. The information gleaned from these forms of analysis can be exploited to **control** the system such that it stays within desired limits.

3 Hybrid Automata

Intuitively, a **Hybrid automaton** (HA) is an extended finite-state automaton, where each state is endowed with a continuous dynamics [17]. Formally, an HA $\mathcal{A} = (X, G, init, inv, flow, jump, event)$ over finite set Σ of **events** is a 7-tuple where:

- A finite set X of real-valued **variables** x_1, \dots, x_n ; their dotted form $\dot{x}_i \in \dot{X}$ represents first derivatives and their primed form $x'_i \in X'$ represents values at the conclusion of discrete steps (jumps); n is called the *dimension* of \mathcal{A} .
- A finite **control graph** $G = (V, E)$, where vertices in V are called *modes* and edges in E are called *switches*.
- Vertex-labeling functions $init$, inv and $flow$ assigned to each mode $v \in V$. Initial condition $init(v)$ and invariant $inv(v)$ are predicates with free variables from X . Flow $flow(v)$ is a predicate with free variables from $X \cup \dot{X}$ representing a set of ordinary (partial) differential (in)equations.
- Edge-labeling functions $jump$ and $event$ assigned to each switch $e \in E$. Jump $jump(e)$ is a predicate with free variables from $X \cup X'$ and is usually divided into a *guard* and an *assignment action*. Event $event(e)$, when defined, is an event in Σ .

The HA \mathcal{A} spends time in its modes $v \in V$, where it updates its variables according to the flow predicate $flow(v)$. Jumps $jump(e)$ on switches $e = (v, w)$ are in contrast instantaneous. A jump on e **may** be taken whenever event $event(e)$ occurs, the jump's guard $jump(e).guard$ is enabled for the current valuation of variables X , and the invariant of the destination mode $inv(w)$ is satisfied after the jump's action $jump(e).action$ is taken. A jump with no associated event is called internal, and taken when all other conditions hold. Invariants are used to **force** a jump, by requiring that a mode v is left before its invariant $inv(v)$ becomes false.

An HA has a natural graphical representation as a state-transition diagram, with control modes as the states and control switches as the transitions. Flows and invariants (predicates within curly

braces) appear within control modes, while jump conditions (in square brackets) and actions appear near the control switches. Continuous variables are written in lower case (x , v , v_x , etc).

As an example, consider HA \mathcal{A} of Figure 1, which models a simple thermostat system. Initially \mathcal{A} is in mode `ModeOFF` with variable x , which represents the current temperature, initialized to 20°C. While \mathcal{A} is in this mode, the heater is off and the temperature drops until it falls below 19°C. At this time, \mathcal{A} **may** jump to mode `ModeON`. The jump is optional until the temperature reaches 18°C, when the jump is enforced. In mode `ModeON`, the heater is on and the temperature rises until it is above 21°C. From this point on, and definitely at the time where the temperature is 22°C, \mathcal{A} may jump back to mode `ModeOFF`.

4 Excitable Cells

Excitable cells include neurons, cardiac cells, skeletal, and smooth muscle cells. In cardiac cells, on each heart beat, an electrical control signal is generated by the sinoatrial node, the heart's internal pacemaking region. Electrical waves then travel along a prescribed path, exciting cells in the main chambers of the heart (atria and ventricles) and assuring synchronous contractions. At the cellular level, the electrical signal is a change in the potential across the cell membrane which is caused by different ion currents flowing through the cell membrane. This electrical signal for each excitation event is known as an **action potential** (AP). Figure 2 shows the AP waveform for a guinea pig ventricular cell.

For non-pacemaking excitable cells, APs are externally triggered events: a cell fires an action potential as an all-or-nothing response to a supra-threshold stimulus, and each AP follows the same sequence of phases and maintains approximately the same magnitude regardless of the applied stimulus. After an initial step-like increase in the membrane potential, an AP lasts for a couple of milliseconds to hundreds of milliseconds in most mammals. During an AP, generally no re-excitation can occur. The early portion of an AP is known as the “absolute refractory period” due to its non-responsiveness to further stimulation. The later portion is known as the “relative refractory period”, during which an altered secondary excitation event is possible if the stimulation strength or duration is raised.

When an excitable cell is subjected to repeated stimuli, two important time periods can be identified: the **action potential duration** (APD), the time the cell is in an excited state, and the **diastolic interval** (DI), the time between the end of the action potential and the next stimulus. Figure 2 illustrates the two intervals. The function relating APD to DI with change in stimulation frequency is called the **APD restitution function**. As shown in Figure 3, the relationship is

nonlinear and captures the phenomenon that a longer recovery time is followed by a longer APD. A physiological explanation of a cell's restitution is rooted in the ion-channel kinetics as a limiting factor in the cell's frequency response.

5 Models of Excitable Cells as Hybrid Automata

During the early stages of the quest for models of excitable cells amenable to analytical investigation, FitzHugh and Nagumo proposed an approximate model of excitable cells [14], referred to here as the FHN model. With their model, they showed that a modified version of the Van der Pol oscillator with two state variables can mimic the essential features of the Hodgkin-Huxley dynamics.

Subsequently, a piecewise-linear version of the FHN model was proposed by McKean [23] which used a **Heaviside function** to represent switches between linear regimes or modes. Since then, the Heaviside function has been used in different simplified renditions of excitable-cell models to achieve piecewise control.

5.1 From Heaviside Control to Hybrid Automata

Discrete transitions in system behavior, such as those captured by Heaviside functions, are an integral part of the HA formalism. Let S be a dynamic system defined using the Heaviside function. Below we present a systematic way to transform S into an equivalent HA. The Heaviside function $H(x)$ is a discontinuous function defined as follows:

$$H(x) = \begin{cases} 0, & x < 0; \\ 1, & x \geq 0. \end{cases} \quad (1)$$

Assuming that the state equation of S has the structure of equations (2), it is straightforward to show that S is equivalent to the HA of Figure 4.

$$\dot{v} = f(H(x), y), \quad \vec{v} = (x, \vec{y}) \quad (2)$$

One can generalize the above translation to any dynamic system whose state equations are defined using Heaviside functions. In the following, we apply this translation to two recently proposed approximate models for cardiac-tissue excitability: the piecewise-linear model of Biktashev [6] and the nonlinear model of Fenton and Karma [13].

5.2 Biktashev's Model

The increasing complexity of excitable-cell models describing AP morphology with large sets of state variables and nonlinear differential equations triggered continuous efforts to obtain simplified descriptions that preserve important properties.

Biktashev made the observation that the widely used FHN model is not sophisticated enough to capture the propagation failure due to dissipation of the wavefront, a phenomenon seen in more realistic models [6]. This was attributed to the more phenomenological nature of the FHN model, which was not directly derived from the original HH model, but rather devised to mimic its properties. Instead, a formal derivation procedure was proposed based on singular perturbation theory developed by Tikhonov and Pontryagin. The procedure reduces the size of the differential equations by taking advantage of the fast-slow nature of the system; i.e. by separating the state variables into two groups, fast-slow, and by linking the two sets of equations via a perturbation parameter. The model thus obtained was able to overcome the above-mentioned deficiency of the original FHN model. Furthermore, its simplicity allowed analytical treatment [6, 26, 7].

Consider Biktashev's simplified model [6] below, where H is the Heaviside function, E is the transmembrane voltage, h is the probability density of a sodium-channel gate being open, D is the (constant) diffusion coefficient, and τ is also constant. \dot{E} and \dot{h} are the time derivatives of state variables E and h , and $\nabla(D\nabla E)$ is the second-order directional derivative on the 2-D space, representing the diffusion factor when modelling the spatial propagation of cell excitations.

$$\dot{E} = \nabla(D\nabla E) + H(E - 1)h \quad (3)$$

$$\dot{h} = \frac{1}{\tau}(H(-E) - h) \quad (4)$$

From the point of view of one cell, $\nabla(D\nabla E)$ is the (input) stimulation current I_s produced by neighboring cells. Hence, equation (3) can be rewritten as follows: $\dot{E} = I_s + H(E - 1)h$. Applying the transformation process for systems employing Heaviside control (see the previous subsection) yields the HA of Figure 5. This HA has three modes, each with flows described by linear time-invariant (LTI) differential equations.

The linearity of the flows is clearly an advantage of this model, as it supports efficient simulation and detailed analysis. However, the simplicity of Biktashev's model comes at a price: the inability to faithfully reproduce AP morphology, as discussed in [6, 7]. This is probably due to the treatment of τ as a constant, when in reality it is a voltage-dependent parameter that can vary over a

relatively wide range. Recently, this piece-wise linear formulation has been augmented with non-Tikhonov asymptotic reduction to obtain a more realistic AP morphology. For example, Biktashev started with the Courtemanche model of the atrial heart cell [8] and applied asymptotic embedding, considering fast and slow variables, to obtain a reduced system [7, 25]. The resultant model captures AP morphology well, but is non-linear in each of the modes separated by a Heaviside function.

5.3 The Fenton-Karma Model

In [13], Fenton and Karma proposed a three-variable ionic model as a substitute for the full ionic LRd-type models, by grouping the various ion currents into three generic ones: fast inward current I_{fi} , slow inward current I_{si} , and slow outward current I_{so} . The corresponding three-variable model below contains dynamic functions for the normalized membrane voltage u , inactivation-activation gate v for I_{fi} , and gate w for I_{si} (the diffusion term is omitted here):

$$\dot{u} = -J_{fi}(u; v) - J_{so}(u) - J_{si}(u; w) \quad (5)$$

$$\dot{v} = H(u_c - u)(1 - v)/\tau_v^- - H(u - u_c)v/\tau_v^+ \quad (6)$$

$$\dot{w} = H(u_c - u)(1 - w)/\tau_w^- - H(u - u_c)w/\tau_w^+ \quad (7)$$

$$J_{fi}(u; v) = -\frac{v}{\tau_d}H(u - u_c)(1 - u)(u - u_c) \quad (8)$$

$$J_{so}(u) = \frac{u}{\tau_o}H(u_c - u) + \frac{1}{\tau_r}H(u - u_c) \quad (9)$$

$$J_{si}(u; w) = -\frac{w}{2\tau_{si}}(1 + \tanh[k(u - u_c^{si})]) \quad (10)$$

where $J_{fi}(u; v)$, $J_{si}(u; w)$, and $J_{so}(u)$ are the normalized versions of $I_{fi}(u; v)$, $I_{si}(u; w)$ and $I_{so}(u)$, respectively; u_c and u_c^{si} are the thresholds for activation of I_{fi} and I_{si} ; τ_v^+ , τ_v^- , τ_w^+ , τ_w^- , τ_d , τ_o , τ_r , and τ_{si} are time constants.

$$\tau_v^-(u) = H(u - u_v)\tau_{v1}^- + H(u_v - u)\tau_{v2}^- \quad (11)$$

$\tau_v^-(u)$ is further defined by the Heaviside function (11), where u_v is the threshold potential and τ_{v1}^- , τ_{v2}^- are time constants.

The Fenton-Karma model recast as an HA is shown in Figure 6. The HA was derived by taking into account the definition of the Heaviside functions and the status of an outside stimulus current $I_{stimulus}$ (omitted in the above equations). The stimulus current is modeled with the aid of two external events, \mathbf{e}_{on} and \mathbf{e}_{off} , signaling the beginning and respectively the end of stimulation.

The Fenton-Karma model has the flexibility to match AP morphology by correct selection of the parameters, possibly via an optimization procedure. It also has been shown to properly model

restitution properties of other more complex models or empirically obtained data. However, similar to Biktashev's asymptotically reduced models, the resultant simplified system is still nonlinear and therefore not particularly well suited to analytic treatment.

6 Cycle-Linear Hybrid Automata for Excitable Cells

In the previous section, we saw that any computational model of excitable cells that employs the Heaviside function for discrete control can be recast as an HA. In particular, Biktashev's simplified model [6] corresponds to an LTI-HA: an HA having linear time-invariant (LTI) flows in each mode. An LTI-HA, such as Biktashev's, is amenable to efficient numerical (or event-driven [27]) simulation as well as formal analysis. Biktashev's simplified model and the corresponding HA are, however, unable to faithfully capture AP morphology.

Biktashev's more sophisticated models and the Fenton-Karma model correspond to HA having nonlinear flows in at least one mode, and faithfully capture AP morphology and restitution properties. Due to the nonlinearity present in these models, however, HA simulation is less efficient and powerful analysis techniques developed for linear systems are not directly applicable.

Given this state of affairs, it is natural to ask the following question: Is it possible to develop an LTI-HA excitable-cell model that is (i) simple enough to be easily understandable and (ii) expressive enough to capture AP morphology and restitution properties? The intrinsic nonlinearity of the restitution property suggests, at first glance, that these goals might be at odds with one another.

Assume for the moment that we give up requirement (i). In this case, we can partition the (multidimensional) phase space of the original nonlinear system into a grid of finite elements such that, for each element, the system is linearly approximated [12]. The resulting finite-element approximation of the system can be viewed as an HA having a mode with LTI flow for each element, and a jump from one mode to another whenever the border between the corresponding elements is crossed. The more elements chosen, the better the approximation but also the larger the number of modes in the HA.

A typical finite-element approximation of a nonlinear system may comprise millions of elements. An important practical question is whether is possible to obtain a "reduced" finite-element HA in which modes (elements) are grouped into a small number of intuitive "generic modes" and the actual modes are computed (instantiated) on the fly? In the rest of this section, we show that such a grouping is possible and that it results in what we call **cycle-linear hybrid automata** (CLHA).

6.1 CLHA Derivation Method

The method we used to derive the CLHA model for excitable cells focuses on the following three issues:

Topology The topology of a CLHA refers to the design of its control graph; i.e. the control graph's modes and mode transitions.

Flows Let \mathcal{A} be a CLHA defined over a set (vector) of state variables X . The dynamics of \mathcal{A} is determined by the dimension of X and, for each mode q of \mathcal{A} , the form of q 's flow (system of ODEs in X).

Adaptability This refers to the mechanism built into the CLHA model that allows it to exhibit stimulation-frequency adaptability. This feature is essential for the successful modelling of AP morphology and restitution.

The discussion of our derivation method proceeds as follows. We first consider the issues of topology and flows, and in the process derive an LTI-HA model \mathcal{A}_1 that approximates the AP trajectory of one representative AP cycle of an excitable cell. We then turn our attention to adaptability. In the process, we derive our final CLHA model \mathcal{A}_2 which offers an accurate approximation of the (infinite-trajectory) phase space of the original nonlinear system.

6.1.1 Topology

The choice of modes for both our LTI-HA \mathcal{A}_1 and CLHA \mathcal{A}_2 models is inspired by the fact that, although the AP for different cell types (neuron, cardiac myocyte, etc.) or different species (guinea pig, neonatal rat, etc.) exhibit different waveforms, when observed over time, one can universally identify the following phases within a cycle: **resting**, **upstroke**, **early repolarization**, **plateau or later repolarization**, and **final repolarization**. Figure 7(a) shows a typical AP cycle for a guinea pig ventricular cell. The voltage thresholds V_T , V_O and V_R serve to delineate one phase of the AP cycle from another.

For the purpose of mode identification, we are also interested in the period of time when an excitable cell is stimulated and can be further subjected to external stimulation. We shall refer to this mode as **stimulated**, and allow the CLHA model to accept input within this mode. This leads us to the following choice of four modes for our CLHA model in order to cover the complete AP cycle: **stimulated (ST)**, **upstroke (UP)**, **early repolarization and plateau (EP)**, and **final repolarization and resting (FR)**. In what follows, we shall typically refer to a mode by its two-letter abbreviation.

As illustrated in Figure 7(b), where flows are momentarily ignored, the mode transition relation for \mathcal{A}_1 and \mathcal{A}_2 is generally cyclic in nature, although we allow the cell to return to mode **FR** from mode **ST** when it is under insufficient stimulus.

Due to its topology, \mathcal{A}_1 and \mathcal{A}_2 already possesses two common features of excitable cells: **absolute refractoriness** and **graded response to sub-threshold stimulation**. Regarding the former, once a cell is excited, e.g., with a stimulus current, it enters an absolute refractory period, where the cell is nonresponsive to further excitation. This is reflected in our models by modes **UP** and **EP**, during which no further input is accepted and the cell cannot return to mode **UP**. Another excitation is possible only when the cell is in **FR**, and is captured with by a begin-stimulation event e_s that moves the model to mode **stimulated**.

Graded response to sub-threshold stimulation happens in mode **ST**, where a cell accumulates its membrane voltage by accepting an input current. As soon as its voltage exceeds threshold V_T , the cell moves to mode **upstroke**. Otherwise, should the end-stimulation event \bar{e}_s occur while $v < V_T$, the cell returns to mode **FR**. This is ultimately a consequence of the refractory modes: if the stimulus occurs at a sufficiently high pace, every second stimulation event may be missed, therefore doubling the cycle period.

6.1.2 Flows

As noted in Section 4, an AP is caused by different ion currents flowing through the cell membrane. There are three major types of ion currents involved: fast inward, outward, and slow inward. We therefore use three state variables $\mathbf{X} = [v_x, v_y, v_z]^T$ to respectively represent the voltage associated with these currents. The equation for the overall membrane voltage v is thus:

$$v = v_x - v_y + v_z \quad (12)$$

The basic idea behind the flows of LTI-HA \mathcal{A}_1 is to capture the nonlinear dynamics (morphology) of a single AP in a piecewise-linear fashion. Since the AP (voltage v) is the only observed variable and we do not have other constraints on the dynamics of state variables, the flows in each mode can be described in a purely linear manner as follows:

$$\dot{\mathbf{X}} = \mathbf{A}\mathbf{X} \quad (13)$$

$\dot{\mathbf{X}}$ refers to the first derivative of \mathbf{X} with respect to time and \mathbf{A} is a constant diagonal matrix. We thus have that the membrane voltage is determined by the independent (as matrix \mathbf{A} is diagonal) contribution of three different types of ion currents. This independency assumption is also seen

in most mathematical ion-current models, where the ion currents are only interconnected by the membrane voltage.

Let $\mathbf{A} = \text{diag}(\alpha_x, \alpha_y, \alpha_z)$. The flows in modes **UP**, **EP** and **FR**, where no input is accepted, are given by:

$$\dot{v}_x = \alpha_x v_x, \quad \dot{v}_y = \alpha_y v_y, \quad \dot{v}_z = \alpha_z v_z \quad (14)$$

Curve-fitting techniques are used to determine parameters α_x , α_y , and α_z in each mode such that the output of the LTI system, i.e. the AP v , reproduces up to a prescribed error margin, the AP of the original system.

By considering a linear dependence on the input in mode **ST**, we still remain within the LTI-HA framework, but are now able to capture a (simplified) family of related trajectories:

$$\dot{v}_x = \alpha_x v_x + \beta_x I_s, \quad \dot{v}_y = \alpha_y v_y + \beta_y I_s, \quad \dot{v}_z = \alpha_z v_z + \beta_z I_s \quad (15)$$

As in the other modes, $\alpha_x, \alpha_y, \alpha_z$ and $\beta_x, \beta_y, \beta_z$ are the constants to be fitted.

6.1.3 Adaptability

The shape of the AP generated by \mathcal{A}_1 is fixed by the constant (matrix and scalar) parameters α , β , V_T , V_O and V_R . Moreover, the APD depends solely on the stimulation frequency, as the time \mathcal{A}_1 spends in modes **ST**, **UP**, and **EP** (for fixed amplitude of I_s) is constant.

In contrast, the original nonlinear system has a phase space comprising infinitely many trajectories. To obtain an accurate approximation of this space, we construct a **cycle-linear hybrid automaton** \mathcal{A}_2 . Before giving a formal definition of the CLHA model, we first show how to derive \mathcal{A}_2 from \mathcal{A}_1 by generalizing \mathcal{A}_1 's constant parameters α , β , V_O and V_T to **cycle-constant** functions $\alpha(\theta)$, $\beta(\theta)$, $V_O(\theta)$ and $V_T(\theta)$, where θ is a normalized one-cycle memory of the voltage. This derivation follows from the following observation:

- APs in different cycles share a similar morphology, making it possible to model them using equations with the same structure.
- According to the restitution property, AP shape is mainly determined by the length of the previous DI. This indicates that a relatively simple (single-step memory) control will be up to the task.

CLHA memory. To accurately capture the DI, one may introduce a timer (a variable whose derivative with respect to time is 1) that is reset when \mathcal{A}_2 enters mode **FR** and measured when

the stimulation event e_s occurs. To maintain only three state variables, we have chosen, however, to linearly approximate the DI with the value of the voltage v of \mathcal{A}_2 at the occurrence of e_s . We remember this value by introducing a discrete variable v_n (its derivative is zero in all modes) that is updated on the transition from **FR** to **ST** with the (assignment) action $v'_n = v$.

To see why the normalized v_n is a linear approximation of the DI, consider the triangles in Figure 8, where DI_m is the maximum value of the DI interval before v becomes zero. The triangle $V_R \ 0 \ DI_m$ is similar to the triangle $N \ DI \ DI_m$ and therefore $v_n/V_R = (DI_m - DI)/DI_m$. Let $\theta = v_n/V_R$ and $\gamma = DI/DI_m$ be the normalized voltage and DI, respectively. Then $\theta = 1 - \gamma$. In the following we let θ play the role of the (normalized) DI .

CLHA shape. The DI in one AP-cycle influences the shape of the AP in the next cycle, in particular, the APD, the stimulation voltage V_T , and the overshoot voltage V_O . The time \mathcal{A}_2 spends in modes **ST** and **UP** is relatively small compared to the APD, thereby allowing the influence of the DI in these modes to be ignored. The time \mathcal{A}_2 spends in modes **EP** and **FR**, however, can be considerable. We therefore make the parameter matrix α a function of θ . Formally, we introduce a new parameter matrix $\bar{\alpha}$ such that:

$$\bar{\alpha}_x(\theta) = \alpha_x f_x(\theta), \quad \bar{\alpha}_y(\theta) = \alpha_y f_y(\theta), \quad \bar{\alpha}_z(\theta) = \alpha_z f_z(\theta), \quad (16)$$

The definitions of f_x , f_y and f_z for these two modes and different cell types are given in Table 1. Note how θ influences the shape of the AP within these two modes. The larger the value of θ , the steeper and therefore the shorter the AP. Moreover, although θ is a linear approximation of the DI, the APD depends on θ (and therefore the DI) in a nonlinear way, as θ appears as the exponent of the analytic solution.

To model the dependency of the threshold voltage V_T and overshoot voltage V_O on the DI, we replace constants V_T and V_O with cycle-constant functions $V_T(\theta)$ and $V_O(\theta)$. Putting everything together, we get the CLHA \mathcal{A}_2 of Figure 9.

6.2 CLHA definition.

We are now ready to give the formal definition of a CLHA. Given an HA $\mathcal{A} = (X, G, init, inv, flow, jump, event)$, we say that \mathcal{A} is **cycle-linear** if the following conditions hold:

- The set of variables X is partitioned into a vector x of continuous variables and a vector θ of discrete variables.
- The control-flow graph $G = (V, E)$ is a cycle. Moreover, vector θ is updated by the *jump* from the initial mode.

- For each mode $v \in V$, $flow(v)$ is an LTI-system of the form $x = \alpha(\theta)x + \beta(\theta)u$ where u is the input. If $\beta(\theta) = 0$ we call v a *refractory* mode.
- For each mode $v \in V$, $inv(v)$ is a (linear) predicate of the form $x \# \gamma(\theta)$, where $\#$ is one of $\{\leq, \geq, <, >\}$ and $\gamma(\theta)$ is a constant vector.
- For each switch $e \in E$, $jump(e).guard$ is a predicate that has the same form as an invariant above.

7 Fitting the CLHA Model to Excitable-Cell Models

In this section, we demonstrate the versatility of the CLHA model by fitting its parameters to successfully capture the AP morphology and restitution of three popular mathematical models of excitable cells: Hodgkin-Huxley (HH) [18], dynamic Luo-Rudy (LRd) [20], and neonatal rat (NNR) [11].

Fitting the flow parameters of the CLHA excitable-cell model to a specific mathematical model involves the following two-step procedure: (1) Using a single representative AP, fit parameters α_w^i , β_w^i , $0 \leq i \leq 3$, $w \in \{x, y, z\}$. (2) Then, using APs obtained under different stimulation frequencies, fix these parameters and fit functions $f(\theta)_w^i$, $0 \leq i \leq 3$, $w \in \{x, y, z\}$.

A simpler, more ad hoc procedure is used for thresholds V_O , V_R , V_T . Consider, for example, the LRd model. In this case, only V_O , the overshoot voltage, varies significantly from AP to AP: it reaches a maximum value of 131.1 when $\theta = 0$, and a minimum value of 50.1 when $\theta = 1$. Choosing $V_O(\theta)$ to be the function $131.1 - 80.1\sqrt{\theta}$ ensures that V_O attains its proper maximum and minimum values over the range of APs used during the fitting process.

Curve fitting was accomplished using the unconstrained nonlinear optimization routines from the MATLAB Optimization Toolbox. Target voltages are derived from numerical simulations of the HH, LRd, and NNR models, and output values from the CLHA model are compared to these at each time step. The goal of the optimization function is to minimize the overall error, which we succeeded in doing with an average error of 1-2mv per time step.

Although the optimization routines we used for curve fitting are completely automatic, the results they produce depend on the initial values manually supplied to them. It is therefore possible that a superior initialization strategy could yield a better fit. The functions and parameters we obtained using our fitting procedure are summarized in Tables 1 and 2.

For a single AP, the comparison of our CLHA model with HH, LRd and NNR is presented in Fig. 10. In the figure, solid lines represent the values obtained via numerical integration of the original nonlinear systems, while the dashed lines represent the values obtained via numerical inte-

	HH	LRd	NNR
$V_T(\theta)$	26	44.5	$39+9.7742\theta$
$V_O(\theta)$	106.5	$131.1-80.1\sqrt{\theta}$	$106.4-133.57\theta^2$
$V_R(\theta)$	30	30	$22+10.1091\theta$
$f_x^0(\theta)$	1	1	$1+\theta$
$f_y^0(\theta)$	1	1	$1+\theta$
$f_z^0(\theta)$	1	1	$1+\theta$
$f_x^3(\theta)$	1	1	1
$f_y^3(\theta)$	1	$0.29e^{62.89\theta} + 0.70e^{-10.99\theta}$	$1+0.5798\theta$
$f_z^3(\theta)$	1	1	1

Table 1: Function definitions for CLHA \mathcal{A}_2 .

	HH	LRd	NNR		HH	LRd	NNR
α_x^0	-0.1770	-0.0087	-0.0647	α_x^2	2.4323	-0.0069	0.3518
α_y^0	-10.7737	-0.1909	-0.0610	α_y^2	3.4556	0.0759	0.0395
α_z^0	-2.7502	-0.1904	-0.0118	α_z^2	2.8111	6.8265	0.0395
α_x^1	0.3399	-0.0236	-0.0473	α_x^3	-1.4569	-0.0332	-0.0087
α_y^1	4.5373	-0.0455	-0.0216	α_y^3	0.0339	0.0280	0.0236
α_z^1	0.0732	-0.0129	-0.0254	α_z^3	-0.9904	0.0020	0.0087
β_x	-3.6051	0.7772	0.7404	β_z	4.9217	0.2766	0.0592
β_y	0.0284	0.0589	0.0869				

Table 2: Parameter values for CLHA \mathcal{A}_2 .

gration of the corresponding CLHA automaton. When the cell is paced with different frequencies, the restitution function of the CLHA model is compared with LRd model in Figure. 11. It can be seen that we obtain a nonlinear dependence consistent with that observed for the nonlinear models and with that observed **in vitro**.

8 Conclusions

We proposed the use of Hybrid Automata (HA) in general, and Cycle-Linear Hybrid Automata (CLHA) in particular, as a general framework for contemporary ion-channel approximation models. Representing the complex response of excitable cells with piecewise-linear HA permits fully analytical solutions in the different phases of the excitation cycle, therefore providing a framework for analytical analysis regardless of system complexity. Additionally, the piecewise linearization

of the system and the simplified description increase computational efficiency without abstracting away essential system features. Moreover, a cycle-linear model of a dynamical system enjoys both the computational efficiency of a linear model and the descriptive power of a nonlinear one, making it more amenable to formal analysis (e.g. stability analysis) than its nonlinear counterpart.

We illustrated the cycle-linear approach by modelling the behavior of excitable cells. In doing so, we succeed in capturing the action-potential morphology and its adaptation to pacing frequency. The method is, however, generally applicable to systems where some level of periodicity plus adaptation is observed. Furthermore, we have shown how to recast two popular approximation models as HA. The graphical representation is easier to understand while still remaining a fully formal model.

Future work includes applying formal analysis to our CLHA models of excitable cells in order to study their fundamental properties, including stability, observability and safety (prevention of arrhythmia). We also plan to investigate techniques for further improving the efficiency of our approach. For example, in some modes of a CLHA model, it is possible to analytically solve the mode's linear differential equations, thereby eliminating the integration steps that would otherwise be required.

9 Acknowledgements

Research supported in part by NSF Grant CCF05-23863 and NSF Career Grant CCR01-33583.

References

- [1] R. Alur, T. Dang, and F. Ivancic. Reachability analysis of hybrid systems via predicate abstraction. In *HSCC*, pages 35–48, 2002.
- [2] R. Alur, R. Grosu, Y. Hur, V. Kumar, and I. Lee. Modular specifications of hybrid systems in CHARON. In *Hybrid Systems: Computation and Control, Third International Workshop*, volume LNCS 1790, pages 6–19, 2000.
- [3] M. Antoniotti, C. Piazza, A. Policriti, M. Simeoni, and B. Mishra. Taming the complexity of biochemical models through bisimulation and collapsing: theory and practice. *Theor. Comput. Sci.*, 325(1):45–67, 2004.

- [4] A. Balluchi, L. Benvenuti, M. D. Di Benedetto, C. Pinello, and A. L. Sangiovanni-Vincentelli. Automotive engine control and hybrid systems: challenges and opportunities. *Proceedings of the IEEE*, 88(7):888–912, July 2000.
- [5] C. Belta, J. Schug, and T. Dang. Stability and reachability analysis of a hybrid model of luminescence in the marine bacterium *vibrio fischeri*. In *40th IEEE conference on Decision and Control*, volume 1, pages 869–874, 2001.
- [6] V. N. Biktashev. A simplified model of propagation and dissipation of excitation fronts. *International Journal of Bifurcation and Chaos*, 13:3605–3619, 2003.
- [7] I. Biktasheva, R. Simitev, R. Suckley, and V. N. Biktashev. Asymptotic properties of mathematical models of excitability. *Philosophical Transactions of the Royal Society A: Mathematical Physical and Engineering Sciences*, 364:1283–1298, 2006.
- [8] M. Courtemanche, R. J. Ramirez, and S. Nattel. Ionic mechanisms underlying human atrial action potential properties: insights from a mathematical model. *Am J Physiol*, 275:301–321, 1998.
- [9] A. Deshpande, D. Godbole, A. Göllü, and P. Varaiya. Design and evaluation of tools for automated highway systems. In *Hybrid Systems III*, LNCS 1066, pages 138–148. Springer-Verlag, 1996.
- [10] J. G. Dumas and A. Rondepierre. Modeling the electrical activity of a neuron by a continuous and piecewise affine hybrid system. In *Hybrid Systems: Computation and Control*, pages 156–171, 2003.
- [11] E. Entcheva and et al. A computation model of the neonatal rat ventricular cell, 2006. Unpublished.
- [12] A. Ern and J.L. Guermond. *Theory and Practice of Finite Elements*. Springer, 2000.
- [13] F. Fenton and A. Karma. Vortex dynamics in 3d continuous myocardium with fiber rotation: Filament instability and fibrillation. *CHAOS*, 8:20–47, 1998.
- [14] R. FitzHugh. Impulses and physiological states in theoretical models of nerve membrane. *Biophys J*, 1:445–467, 1961.

- [15] R. Ghosh and C. J. Tomlin. Lateral inhibition through delta-notch signaling: A piecewise affine hybrid model. In *Hybrid Systems: Computation and Control : 4th International Workshop*, volume 2034 of *Lecture Notes in Computer Science*, Rome, Italy, March 2001. Springer-Verlag.
- [16] R. Ghosh and C. J. Tomlin. Symbolic reachable set computation of piecewise affine hybrid automata and its application to biological modeling: Delta-notch protein signaling. *IEEE Transactions on Systems Biology*, 1(1):170–183, June 2004.
- [17] T. A. Henzinger. The theory of hybrid automata. In *Proceedings of the 11th IEEE Symposium on Logic in Computer Science*, pages 278–293, 1996.
- [18] A. L. Hodgkin and A. F. Huxley. A quantitative description of membrane currents and its application to conduction and excitation in nerve. *J Physiol*, 117:500–544, 1952.
- [19] C. Livadas, J. Lygeros, and N. A. Lynch. High-level modelling and analysis of tcas. In *Proceedings of the IEEE Real-Time Systems Symposium*, pages 115–125, 1999.
- [20] C. H. Luo and Y. Rudy. A dynamic model of the cardiac ventricular action potential: I. simulations of ionic currents and concentration changes. *Circ Res*, 74:1071–1096, 1994.
- [21] J. Lygeros, G. J. Pappas, and S. Sastry. An approach to the verification of the center-tracon automation system. In *HSCC '98: Proceedings of the First International Workshop on Hybrid Systems*, pages 289–304, London, UK, 1998. Springer-Verlag.
- [22] O. Maler and S. Yovine. Hardware timing verification using kronos. In *7th IEEE Israeli Conference on Computer Systems and Software Engineering*, June 12-13. IEEE Computer Society Press, 1996.
- [23] H. P. McKean. Nagumo's equation. *Advances in Mathematics*, 4:209–223, 1970.
- [24] R. Milner. *Communication and Concurrency*. International Series in Computer Science. Prentice Hall, 1989.
- [25] R. D. Simitev and V. N. Biktashev. Conditions for propagation and block of excitation in an asymptotic model of atrial tissue. *Biophysical Journal*, 90:2258–2269, 2006.
- [26] R. Suckley and V. N. Biktashev. Comparison of asymptotics of heart and nerve excitability. *Physical Review E*, 68, 2003.
- [27] M. True, E. Entcheva, S. A. Smolka, P. Ye, and R. Grosu. Efficient event-driven simulation of excitable hybrid automata. In *Proceedings of EMBC*, 2006.

- [28] P. Varaiya. Smart cars on smart roads: problems of control. *IEEE Trans. Automatic Control*, 38(2), 1993.

10 Figures

Figure. 1: A thermostat system modeled as an HA.

Figure. 2: The AP and its APD and DI time periods.

Figure. 3: APD dependence on DI in LRd model.

Figure. 4: Heaviside function recast as an HA.

Figure. 5: Biktashev's model in the HA framework.

Figure. 6: HA for the Fenton-Karma 3-variable 3-ion-current model.

Figure. 7: (a) Major AP phases. (b) Structure of CLHA model.

Figure. 8: DI linearization.

Figure. 9: CLHA model of excitable cells.

Figure. 10: AP comparison of CLHA with: (a) HH (b) LRd (c) NNR.

Figure. 11: Restitution comparison with LRd.

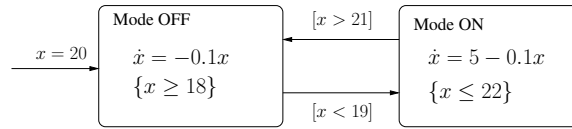


Figure 1: A thermostat system modeled as an HA.

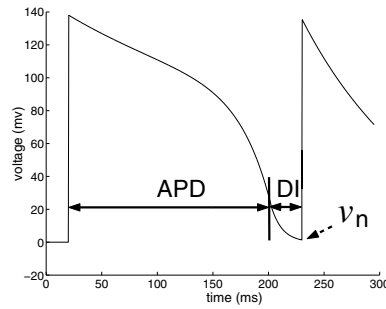


Figure 2: The AP and its APD and DI time periods.

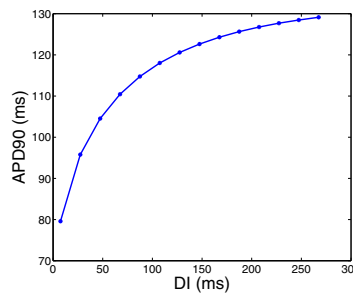


Figure 3: APD dependence on DI in LRd model.

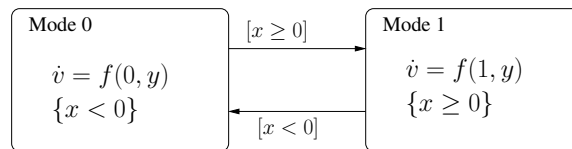


Figure 4: Heaviside function recast as an HA.

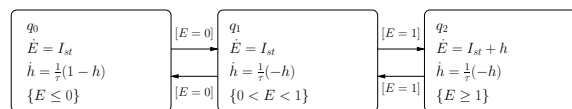


Figure 5: Biktashev's model in the HA framework.

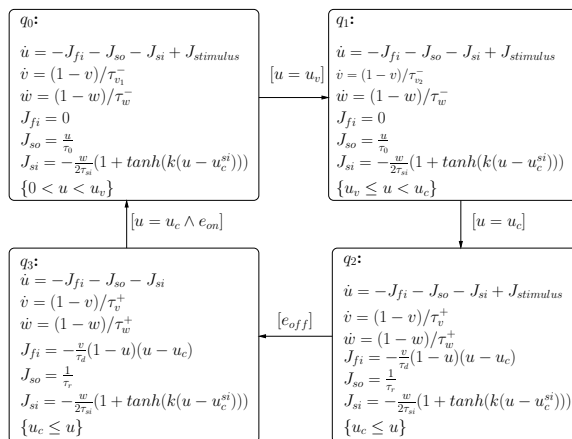
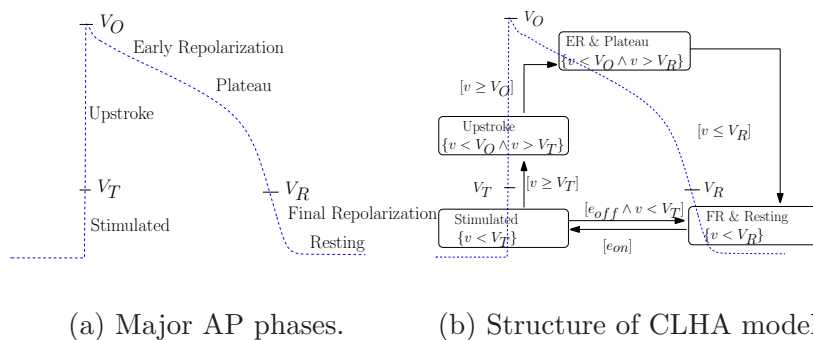


Figure 6: HA for the Fenton-Karma 3-variable 3-ion-current model.



(a) Major AP phases. (b) Structure of CLHA model.

Figure 7:

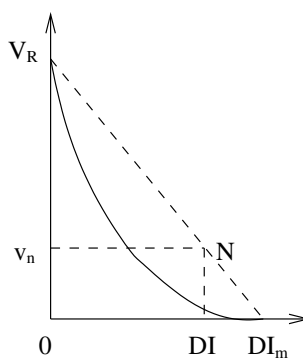


Figure 8: DI linearization.

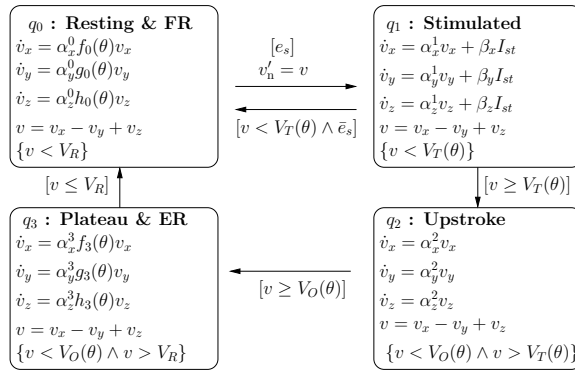


Figure 9: CLHA model of excitable cells.

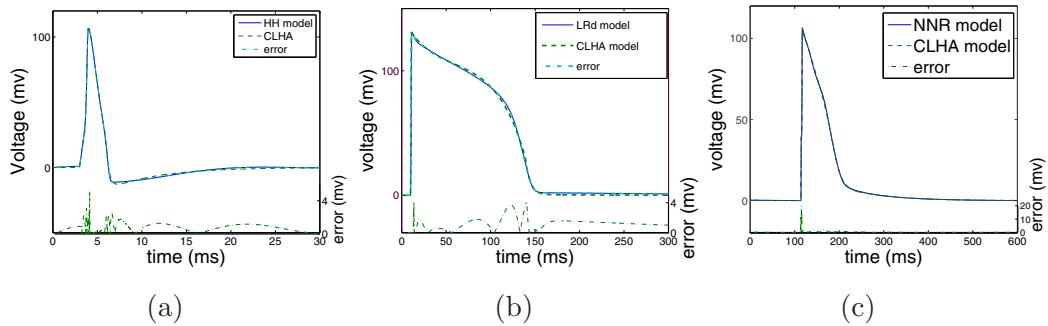


Figure 10: AP comparison of CLHA with: (a) HH (b) LRd (c) NNR

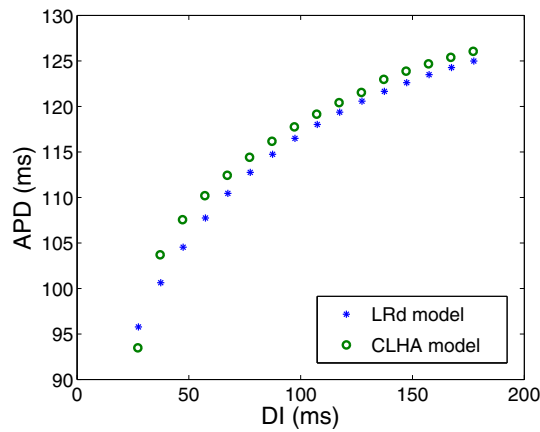


Figure 11: Restitution comparison with LRd.